

# Model-independent reconstruction of $f(T)$ teleparallel cosmology

Salvatore Capozziello,<sup>1,2,3,\*</sup> Rocco D’Agostino,<sup>4,5,†</sup> and Orlando Luongo<sup>1,2,6,7,8,‡</sup>

<sup>1</sup>*Dipartimento di Fisica, Università di Napoli “Federico II”, Via Cinthia, I-80126, Napoli, Italy.*

<sup>2</sup>*Istituto Nazionale di Fisica Nucleare (INFN), Sez. di Napoli, Via Cinthia 9, I-80126 Napoli, Italy.*

<sup>3</sup>*Gran Sasso Science Institute, Via F. Crispi 7, I-67100, L’Aquila, Italy.*

<sup>4</sup>*Dipartimento di Fisica, Università degli Studi di Roma “Tor Vergata”,  
Via della Ricerca Scientifica 1, I-00133, Roma, Italy.*

<sup>5</sup>*Istituto Nazionale di Fisica Nucleare (INFN), Sez. di Roma “Tor Vergata”,  
Via della Ricerca Scientifica 1, I-00133, Roma, Italy.*

<sup>6</sup>*School of Science and Technology, University of Camerino, I-62032, Camerino, Italy.*

<sup>7</sup>*Department of Mathematics and Applied Mathematics,  
University of Cape Town, Rondebosch 7701, Cape Town, South Africa.*

<sup>8</sup>*Astrophysics, Cosmology and Gravity Centre (ACGC),  
University of Cape Town, Rondebosch 7701, Cape Town, South Africa.*

(Dated: March 5, 2018)

We propose a model-independent formalism to numerically solve the modified Friedmann equations in the framework of  $f(T)$  teleparallel cosmology. Our strategy is to expand the Hubble parameter around the redshift  $z = 0$  up to a given order and to adopt cosmographic bounds as initial settings to determine the corresponding  $f(z) \equiv f(T(H(z)))$  function. In this perspective, we distinguish two cases: the first expansion is up to the jerk parameter, the second expansion is up to the snap parameter. We show that inside the observed redshift domain  $z \leq 1$ , only the net strength of  $f(z)$  is modified passing from jerk to snap, whereas its functional behavior and shape turn out to be identical. As first step, we set the cosmographic parameters by means of the most recent observations. Afterwards, we calibrate our numerical solutions with the concordance  $\Lambda$ CDM model. In both cases, there is a good agreement with the cosmological standard model around  $z \leq 1$ , with severe discrepancies outer of this limit. We demonstrate that the effective dark energy term evolves following the test-function:  $f(z) = \mathcal{A} + \mathcal{B}z^2 e^{Cz}$ . Bounds over the set  $\{\mathcal{A}, \mathcal{B}, \mathcal{C}\}$  are also fixed by statistical considerations, comparing discrepancies between  $f(z)$  with data. The approach opens the possibility to get a wide class of test-functions able to frame the dynamics of  $f(T)$  without postulating any model *a priori*. We thus re-obtain the  $f(T)$  function through a back-scattering procedure once  $f(z)$  is known. We figure out the properties of our  $f(T)$  function at the level of background cosmology, to check the goodness of our numerical results. Finally, a comparison with previous cosmographic approaches is carried out giving results compatible with theoretical expectations.

## I. INTRODUCTION

A challenge of modern cosmology is to determine how the universe constituents precisely affect the dynamics as the universe expands. In particular, at late times of its evolution, the universe seems to be dominated by an exotic fluid dubbed dark energy, whose origin is so far unknown [1]. A wide number of observations points out that dark energy should act as a fluid with negative pressure counterbalancing the action of gravity, and speeding up the universe after a transition epoch [2, 3]. The standard approach which most likely aims to describe such a dynamics assumes that the source of dark energy is supplied by a non-zero cosmological constant  $\Lambda$ , associated to vacuum quantum field fluctuations [4]. The paradigm which makes use of  $\Lambda$  is referred to as the  $\Lambda$ CDM concordance model and represents the simplest approach describing the observed universe dynamics [5].

Although well-supported by observations, the concor-

dance model does not give explanations towards the *coincidence problem* [6] between dark matter and dark energy orders of magnitude and the *fine-tuning* issue between predictions of quantum gravity and today observational constraints on the value of  $\Lambda$  [7]. Hence, a possible alternative interpretation is that the fluid which triggers the current universe speed up may not be due to  $\Lambda$ . For example, one can conclude that the effect of cosmic acceleration may be obtained in the framework of modified gravities where extensions of General Relativity (GR) are accounted. In any gravitational theory which extends GR, additional degrees of freedom could be interpreted as dark energy sources [8, 9].

In the context of modified gravity, it is possible to replace the Ricci scalar  $R$  in the Einstein-Hilbert action by arbitrary functions of  $R$  and any curvature invariant giving rise to Extended Theories of Gravity [8, 10, 11]. However a torsional formulation of GR, namely the *Teleparallel Equivalent of General Relativity* (TEGR) [12] is also possible. In this approach, the gravitational action is given by the torsion scalar  $T$  and one can construct the  $f(T)$  extension of TEGR [13–15], where  $f(T)$  is a function of  $T$ . The predictions of GR turn out to coincide with TEGR, whereas the same does not happen for  $f(T)$

\* capozziello@na.infn.it

† rocco.dagostino@roma2.infn.it

‡ luongo@na.infn.it

with respect to  $f(R)$  gravity [15]. Indeed,  $f(T)$  models lead to different outcomes if compared with the corresponding  $f(R)$  approach. For these reasons, the  $f(T)$  formulation of gravity represents an interesting approach with a significative number of cosmological implications which are today object of intensive investigation [14–17].

In this paper we are going to investigate a model-independent approach to reconstruct the  $f(T)$  function from cosmological observations. In this perspective, we consider the cosmological Friedmann equations for a generic analytical  $f(T)$  function. Afterwards, we recast the corresponding equations in terms of the redshift and Hubble parameter  $H(z)$ . In so doing, we obtain a differential equation which can be numerically solved, once  $H(z)$  is somehow fixed by data. Even though we are interested in reconstructing  $f(T)$ , if we impose parametric forms of  $H(z)$  we would fix the model *a priori*, influencing our numerical analyses which turn out to be model dependent. To overcome this problem, we expand  $H(z)$  in Taylor series around  $z \simeq 0$ , which corresponds to present time  $t_0$ . Since cosmography or cosmo-kinetics lie on expansions of  $a(t)$  around  $t = t_0$ , our expansions of  $H$  can be related to the cosmographic parameters, as in the case of  $a(t)$ . In particular, we consider two expansions: the former considering the cosmographic parameters  $H_0, q_0$  and  $j_0$ , while the latter considering also the snap parameter  $s_0$ . In such a picture, the cosmographic series does not require the assumption of any model *a priori*. So that, using the most recent bounds over the cosmographic parameters, we are able to model-independently reconstruct  $f(T)$ . In fact, it is possible to demonstrate that the above set of parameters univocally defines the shapes of  $f(T)$  in the interval  $0 < z < 2$ . Furthermore, being  $f(T) = f(H(z))$ , it is possible to set a direct correspondence between  $f(T)$  and  $f(z)$ . The former,  $f(z)$ , can be easily matched with arbitrary functions of the redshift  $z$ . Thus, we first reconstruct  $f(z)$  by means of the cosmographic data and afterwards we come back to  $f(T)$  and its evolution in terms of  $T$ .

In both cases, we find a good agreement between the predicted and recovered shapes of  $f(z)$  and  $f(T)$  and it is possible to notice that curve strengths are only modified, leaving unaltered the functional behaviors of each curves. To figure out this result, we numerically analyze the obtained curves with a class of test-functions. We conclude that the best approach is offered by a particular class of combined exponential functions. With these considerations in mind, we obtain the corresponding  $f(T)$  and study the background cosmology. In particular, it is possible to describe the effective dark energy term and its evolution in time. Finally, it is possible to fix limits over the equation of state (EoS) and achieve a form for  $f(T)$  which well adapts to cosmic evolution at late times.

The layout of the paper is the following. In Sec. II we briefly summarize the main ingredients of  $f(T)$  teleparallel gravity and cosmology. In Sec. III, the basic requirements to solve numerically the modified Friedmann equations are discussed. In particular, the standard issues of

cosmography are considered and the main reasons to conclude that cosmography is a model-independent approach to frame the universe dynamics are discussed. In Sec. IV, the method for numerically solving the Friedmann equations is implemented and solutions for  $f(z)$  and  $f(T)$  are introduced. Sec. V is devoted to the investigation of the obtained  $f(T)$  models and, in Sec. VI, we compare our results with previous ones obtained in cosmography. Sec. VII is devoted to conclusions and perspectives.

## II. $f(T)$ GRAVITY AND COSMOLOGY

The equations of motion in  $f(T)$  gravities can be derived using as dynamical variables the vierbein fields  $e_A(x^\mu)$ , which form an orthonormal basis for the tangent space at each point  $x^\mu$  of a generic manifold<sup>1</sup>. Introducing the dual basis  $e^A(x^\mu)$ , the metric tensor reads [12]

$$g_{\mu\nu} = \eta_{AB} e_\mu^A e_\nu^B, \quad (1)$$

where  $\eta_{AB} = \text{diag}(1, -1, -1, -1)$  is the Minkowski metric of tangent space. The torsion tensor can be expressed by the zero-curvature Weitzenböck connections  $\hat{\Gamma}_{\mu\nu}^\lambda$  as [15]

$$T_{\mu\nu}^\lambda \equiv \hat{\Gamma}_{\mu\nu}^\lambda - \hat{\Gamma}_{\nu\mu}^\lambda = e_A^\lambda (\partial_\mu e_\nu^A - \partial_\nu e_\mu^A). \quad (2)$$

A convenient choice is to introduce the tensor

$$S_\rho{}^{\mu\nu} = \frac{1}{2} (K^{\mu\nu}{}_\rho + \delta_\rho^\mu T^{\alpha\nu}{}_\alpha - \delta_\rho^\nu T^{\alpha\mu}{}_\alpha), \quad (3)$$

where

$$K^{\mu\nu}{}_\rho = -\frac{1}{2} (T^{\mu\nu}{}_\rho - T^{\nu\mu}{}_\rho - T_\rho{}^{\mu\nu}) \quad (4)$$

is the contorsion tensor. Hence, one can write the torsion scalar, which represents the teleparallel Lagrangian density, in the compact form

$$T = S_\rho{}^{\mu\nu} T^\rho{}_{\mu\nu}. \quad (5)$$

Generalizing to a generic function of  $T$  means that the gravity action can be rewritten as:

$$S = \int d^4x e \left[ \frac{f(T)}{2\kappa} + \mathcal{L}_m \right], \quad (6)$$

where  $e = \sqrt{-g} = \det(e_\mu^A)$  and  $\kappa = 8\pi G$ . We will assume throughout the paper the physical units with  $\kappa = 1$ .  $\mathcal{L}_m$  is the Lagrangian density of the matter fields. The field equations are thus obtained by varying the action (6) with respect to the vierbein fields:

$$\begin{aligned} e_A^\rho S_\rho{}^{\mu\nu} (\partial_\mu T) f'' + \left[ \frac{1}{e} \partial_\mu (e e_A^\rho S_\rho{}^{\mu\nu}) - e_A^\lambda T^\rho{}_{\mu\lambda} S_\rho{}^{\nu\mu} \right] f' \\ + \frac{1}{4} e_A^\nu f = \frac{\kappa}{2} e_A^\rho T^{(m)\nu}{}_\rho \end{aligned} \quad (7)$$

<sup>1</sup> Here, we use the capital Latin indices to denote the coordinate of the tangent space-time, while the Greek letters indicate the coordinates of the manifold.

where  $T^{(m)}{}_{\rho}{}^{\nu}$  represents the energy-momentum tensor of matter. In the above relations, the primes indicate derivatives with respect to  $T$ .

Hence, assuming the validity of the cosmological principle [18], we consider the homogeneous and isotropic Friedmann-Lemaître-Robertson-Walker (FLRW) metric for a spatially flat universe<sup>2</sup>,

$$ds^2 = dt^2 - a^2(t) [dr^2 + r^2(d\theta^2 + \sin^2\theta d\phi^2)] , \quad (8)$$

which corresponds to take the vierbein as:  $e_A^\mu = \text{diag}(1, a, a, a)$ . The modified Friedmann equations are thus [19]:

$$H^2 = \frac{1}{3}(\rho_m + \rho_T) , \quad (9a)$$

$$2\dot{H} + 3H^2 = -\frac{1}{3}(p_m + p_T) , \quad (9b)$$

where  $\rho_m$  and  $p_m$  represent the matter density and pressure for a perfect fluid source. In particular, we assume:

- dark matter and dark energy do not interact between them;
- the matter density,  $\rho_m$ , scales as in standard cosmology, i.e.  $\rho_m \propto a^{-3}$  with  $a = (1+z)^{-1}$ ;
- the matter pressure is  $p_m = 0$  to guarantee a pressureless counterpart composed by baryons and cold dark matter;
- radiation, neutrinos, gravitational relics and so forth are negligibly small at our time and cannot be considered in our analyses,

which turn out to be the basic demands of any cosmological theory to be consistent with current observations. Moreover, in our picture  $\rho_T$  and  $p_T$  are the torsion density and pressure respectively:

$$\rho_T = T f'(T) - \frac{f(T)}{2} - \frac{T}{2} , \quad (10a)$$

$$p_T = \frac{f - T f'(T) + 2T^2 f''(T)}{2[f'(T) + 2T f''(T)]} . \quad (10b)$$

They are clearly zero for  $f(T) = T$ . One can define an “effective” dark energy torsional component, whose EoS takes the standard form in the hydrodynamic approach to cosmology [20]. Since, for each species one has:

$$\omega_i \equiv \frac{p_i}{\rho_i} , \quad (11)$$

<sup>2</sup> Generalizing from spatially flat to non-flat is straightforward. However, spatial curvature would influence the cosmographic analysis, as we will discuss in Sec. III. In this paper we limit our attention to the flat case only.

and

$$\omega_{tot} \equiv \sum_i \left( \frac{p_i}{\rho_i} \right) , \quad (12)$$

then one gets:

$$\omega_{DE} = -1 + \frac{(f - 2T f')(f' + 2T f'' - 1)}{(f + T - 2T f')(f' + 2T f'')} , \quad (13)$$

where we assumed

$$\omega_{DE} \equiv \frac{p_T}{\rho_T} . \quad (14)$$

It can be interpreted as the torsional counterpart of  $f(T)$  giving rise to dark energy effect. Depending on the form of  $f(T)$ , it can be the origin of today observed acceleration of the Hubble flow. Using Eqs. (10a) and (10b), the Friedmann equations can be rewritten as [22]

$$H^2 = -\frac{1}{12f'(T)} [T\Omega_m + f(T)] , \quad (15a)$$

$$\dot{H} = \frac{1}{4f'(T)} [T\Omega_m - 4H\dot{T}f''(T)] , \quad (15b)$$

where  $\Omega_m$  is the normalized matter density parameter whose functional form scales as:  $\Omega_m \equiv \Omega_{m0} a^{-3}$ , with  $\Omega_{m0}$  the current value as measured by observations. In the FLRW universe, the torsion scalar  $T$  obeys the following constraint:

$$T = -6H^2 , \quad (16)$$

which relates the torsion directly with the Hubble parameter at all stages of the universe evolution. With these considerations in mind, in the next paragraph, we rewrite the Friedmann equations as function of the redshift  $z$  and  $H$  finding the  $f(T)$  form, once  $H(z)$  is constrained by cosmography.

### III. $f(T)$ COSMOGRAPHY

Let us highlight now some basic assumptions of cosmography in view of modeling the dynamics of  $f(T)$  [23]. The expansion of scale factor  $a(t)$  in Taylor series around the present time  $t_0$  [24] is

$$a(t) = 1 + \sum_{k=1}^{\infty} \frac{1}{k!} \frac{d^k a}{dt^k} \Big|_{t=t_0} (t - t_0)^k . \quad (17)$$

From this expansion, one defines

$$H \equiv \frac{1}{a} \frac{da}{dt} , \quad q \equiv -\frac{1}{aH^2} \frac{d^2 a}{dt^2} \quad (18)$$

$$j \equiv \frac{1}{aH^3} \frac{d^3 a}{dt^3} , \quad s \equiv \frac{1}{aH^4} \frac{d^4 a}{dt^4} \quad (19)$$

named *Hubble*, *deceleration*, *jerk* and *snap* parameters, respectively. The luminosity distance can be written in terms of the redshift  $z = a^{-1} - 1$  as [25]

$$d_L(z) = (1+z) \int_0^z \frac{dz'}{H(z)}. \quad (20)$$

We can expand in series Eq. (20) by simply plugging Eq. (17) in it and then, by using the cosmographic parameters Eqs. (18)–(19) evaluated at our epoch, obtaining [26]:

$$d_L(z) = \frac{1}{H_0} (c_1 z + c_2 z^2 + c_3 z^3 + c_4 z^4) + \mathcal{E}. \quad (21)$$

Here,  $\mathcal{E}$  is the error associated to the truncation of the series at a given order. In particular, indicating with  $\delta_i$  the errors over the cosmographic coefficients, one gets:

$$\begin{cases} \mathcal{E} \rightarrow 0, & N \rightarrow \infty; \\ \delta \rightarrow \infty, & N \rightarrow \infty. \end{cases} \quad (22)$$

with  $N$  the order of truncating series. The consequences of such requests are that cosmography cannot be used with an arbitrary precision to frame the universe dynamics since any expansions is jeopardized by severe degeneracies among coefficients<sup>3</sup>. This is not the only limit of cosmography but in this work we do not need to discriminate among models when  $N$  significantly increases, but we only require cosmography to guarantee that  $H$  is featured in a model-independent way [28]. Thus, up to the fourth order, as reported in Eq. (21), one gets:

$$\begin{aligned} c_1 &= 1, & c_2 &= \frac{1}{2}(1 - q_0), \\ c_3 &= -\frac{1}{6}(1 - q_0 - 3q_0^2 + j_0), \\ c_4 &= \frac{1}{24}(2 - 2q_0 - 15q_0^2 - 15q_0^3 + 5j_0 + 10q_0 j_0 + s_0). \end{aligned} \quad (23)$$

Hence, using Eq. (20) one can relate the Hubble parameter to the luminosity distance by means of

$$H(z) = \left[ \frac{d}{dz} \left( \frac{d_L(z)}{1+z} \right) \right]^{-1}, \quad (24)$$

and so, making use of Eq. (21), one finds out the Taylor series expansion of  $H$  as a function of the cosmographic parameters:

$$\frac{H(z)}{H_0} = 1 + \sum_{\tilde{k}=1}^{\infty} \frac{1}{\tilde{k}!} \left. \frac{d^{\tilde{k}} H}{dz^{\tilde{k}}} \right|_{z=0} z^{\tilde{k}}, \quad (25)$$

where  $\tilde{k} \neq k$ , while the first three orders read [29]

$$\begin{aligned} \left. \frac{dH}{dz} \right|_{z=0} &= 1 + q_0, \\ \left. \frac{d^2 H}{dz^2} \right|_{z=0} &= j_0 - q_0^2, \\ \left. \frac{d^3 H}{dz^3} \right|_{z=0} &= \frac{1}{6} (j_0(3 + 4q_0) - 3q_0(1 + q_0) + s_0). \end{aligned} \quad (26)$$

Now, if the values of the parameters ( $H_0, q_0, j_0, s_0$ ) are known, one can combine Eqs. (15a) and (15b) to numerically infer the function  $f(T(z)) = f(z)$ . To figure out this point, we need to convert time derivatives and derivatives with respect to  $T$  into derivatives with respect to the redshift  $z$ . For any redshift-dependent function  $\mathfrak{F}(z)$ , it is [30]:

$$\frac{d}{dt} \mathfrak{F}(z) = -(1+z)H(z) \frac{d}{dz} \mathfrak{F}(z), \quad (27)$$

$$\frac{\partial}{\partial T} \mathfrak{F}(z) = -12H(z)H'(z) \frac{d}{dz} \mathfrak{F}(z) \quad (28)$$

where in the latter equation we have used Eq. (16). We will use Eqs. (27) and (28) in what follows, in order to get the forms of the functions  $f(z)$  and  $f(T)$ .

#### IV. NUMERICAL RECONSTRUCTIONS OF $f(T)$ FUNCTION

In this section we want to reconstruct the form of  $f(z)$  by using the requirements imposed in the modified Friedmann equations. To do so, let us consider Eqs. (9a) and (27) which give the following differential equation in terms of  $z$  and  $H(z)$ :

$$\left( \frac{df}{dz} \right)^{-1} \left[ H(1+z) \frac{d^2 f}{dz^2} + 3f \frac{dH}{dz} \right] = \mathcal{D} \quad (29)$$

with

$$\mathcal{D} \equiv \frac{1}{H} \left( \frac{dH}{dz} \right)^{-1} \left[ 3 \frac{dH}{dz} + (1+z) \frac{d^2 H}{dz^2} \right]. \quad (30)$$

As one can soon notice, Eq. (29) depends upon  $z$  and  $H(z)$ . Assuming the form of  $H(z)$  leads to impose the model and to force the consequent analysis. In other words, assuming a given  $H(z)$ , for example the one of the concordance  $\Lambda$ CDM model, would force  $f(z)$  to be compatible with a slightly evolving dark energy term. Since we are looking for reconstructing the Hubble flow at different stages as model-independent as possible, we make use of cosmography to take  $H$  free from any assumptions. Indeed, once the form of  $H(z)$  is reconstructed by Eq. (25), we obtain a model-independent procedure which relates Eq. (29) to  $z$  only, without passing through postulating the cosmological model. In particular, Eq. (29) is a second-order differential equation which

<sup>3</sup> For additional details see [27]

requires two initial conditions over  $f$  and  $\frac{df}{dz}$ . On the one hand, the initial condition on  $\frac{df}{dz}$  can be obtained imposing that the present value of the effective gravitational constant is set to be the Newton constant  $G$  [21, 22]:

$$\left. \frac{df}{dz} \right|_{z=0} = 1. \quad (31)$$

On the other hand, the initial condition over  $f(z)$  comes from Eqs. (16) and (31):

$$f(T(z=0)) = f(z=0) = 6H_0^2(\Omega_{m0} - 2). \quad (32)$$

Moreover, following the strategy in [31], we may recast the cosmographic parameters  $(q_0, j_0, s_0)$  as [32]:

$$q_0 = -1 + \frac{3\tilde{\Omega}_{m0}}{2(1 + 2\tilde{F}_2)}, \quad (33)$$

$$j_0 = 1 - \frac{9\tilde{\Omega}_{m0}^2(3\tilde{F}_2 + 2\tilde{F}_3)}{2(1 + 2\tilde{F}_2)^3}, \quad (34)$$

$$s_0 = 1 - \frac{9\tilde{\Omega}_{m0}}{2(1 + 2\tilde{F}_2)} + \frac{45\tilde{\Omega}_{m0}^2(3\tilde{F}_2 + 2\tilde{F}_3)}{2(1 + 2\tilde{F}_2)^3} + \frac{27\tilde{\Omega}_{m0}^3(3\tilde{F}_2 + 12\tilde{F}_3 + 4\tilde{F}_4)}{4(1 + 2\tilde{F}_2)^4} - \frac{81\tilde{\Omega}_{m0}^3(3\tilde{F}_2 + 2\tilde{F}_3)^2}{2(1 + 2\tilde{F}_2)^5} \quad (35)$$

with

$$\tilde{\Omega}_{m0} = \frac{\Omega_{m0}}{F_1}, \quad \tilde{F}_i = \frac{F_i}{F_1} \quad (i = 2, 3, 4) \quad (36)$$

$$F_i = T_0^{i-1} f^{(i)}(T_0) \quad (i = 1, 2, 3, 4). \quad (37)$$

With those assumptions in mind, we adopt the indicative values reported below [31]:

$$\begin{cases} \Omega_{m0} = 0.289 \\ h = 0.692 \\ q_0 = -0.545 \\ j_0 = 0.776 \\ s_0 = -0.192 \end{cases} \quad (38)$$

where  $h \equiv H_0/(100 \text{ km/s/Mpc})$ . These results are compatible with the current expectations over the cosmographic set of parameters using different data sets [33].

Thus, we handle the aforementioned limits over the cosmographic parameters to numerically solve Eq. (29). To do so, we perform a two-step analysis. In particular, we first consider the Hubble rate expansion up to the second order in  $z$ , namely up to the jerk parameter. We then show our results in Fig. 1 for different values of the set  $(\Omega_{m0}, q_0, j_0)$ , holding  $H_0$  to be fixed.

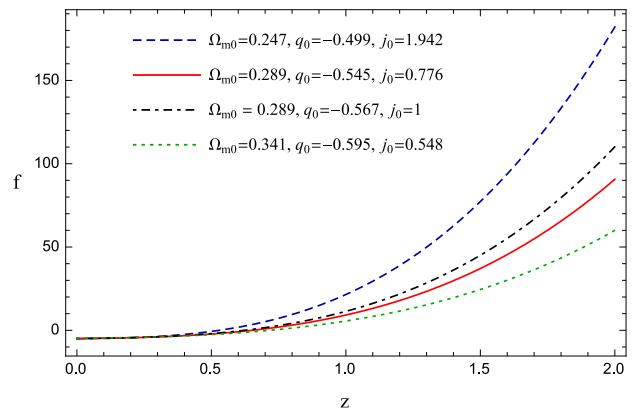


FIG. 1. Numerical reconstruction of  $f(z)$  for different  $(\Omega_{m0}, q_0, j_0)$  based on the results of Table 6 in [31]. The solid red, the dashed blue and the dotted green lines correspond, respectively, to the the best-fit values, the upper  $2\sigma$  bounds and the lower  $2\sigma$  bounds of the parameters  $(\tilde{\Omega}_{m0}, \tilde{F}_2, \tilde{F}_3)$ . The dot-dashed black line corresponds to the  $\Lambda$ CDM model.  $h$  is fixed to the best-fit value of 0.692.

We then match the numerical behaviours using the following test-functions<sup>4</sup>:

$$f_1(z) = \mathcal{A} + z(\mathcal{B} + \mathcal{C}z) \ln(1 + z^2) \quad (39a)$$

$$f_2(z) = \mathcal{A} + \mathcal{B}z^2 e^{\mathcal{C}z} \quad (39b)$$

$$f_3(z) = \mathcal{A}z^2 + \mathcal{B}z \sin(1 + \mathcal{C}z^2) \quad (39c)$$

$$f_4(z) = \mathcal{A} + \mathcal{B}z^2 \cos(1 + \mathcal{C}z) \quad (39d)$$

$$f_5(z) = \mathcal{A} + \mathcal{B} \sinh(1 + \mathcal{C}z) \quad (39e)$$

$$f_6(z) = \mathcal{A} + \mathcal{B}z^3 \tanh(\mathcal{C}z^2) \quad (39f)$$

with  $\mathcal{A}$ ,  $\mathcal{B}$  and  $\mathcal{C}$  free coefficients to be fixed from a direct comparison with the numerical curves. To get suitable outcomes, we find a good analytical approximation according to the following requirements.

- The function  $f(z)$  has to be neither odd nor even.
- The linear term, i.e.  $f(z) \sim z$ , is not favored and does not contribute significantly around the sphere  $z \leq 2$ .
- Cosmography does not influence the functional analysis but rather it fixed the strengths of any test-function. The limits of cosmography are evident, since enlarging the prior domains leads to anomalous results on the form of  $f(z)$  which are not compatible with current dark energy behaviour.

<sup>4</sup> Here, test-functions are used to match *a posteriori* the shapes of numerical curves obtained from our numerical analysis. The forms of such functions have been chosen analysing the shapes and checking any formal trends of the involved curves.

- The  $f(z)$  results are all compatible with the concordance paradigm, but do not exclude dark energy to vary.
- The numerical analyses do not depend upon adding scalar curvature and radiation.

To find, among the test-functions, the best approximation for  $f(z)$ , we perform the  $\mathcal{R}^2$ -test [34]. Denoting by  $f_i^{obs}$  the values of  $f(z_i)$  obtained from the numerical solution, and by  $f_i$  the correspondent values, we can define

$$\mathcal{R}^2 \equiv 1 - \frac{\sum_{i=1}^n (f_i^{obs} - f_i)^2}{\sum_{i=1}^n (f_i^{obs} - \bar{f})^2}, \quad (40)$$

where

$$\bar{f} = \frac{1}{n} \sum_{i=1}^n f_i^{obs} \quad (41)$$

and  $n$  is the number of points. The  $\mathcal{R}^2$  statistics provides information on how well the test-functions approximate the numerical  $f(z)$ , being  $\mathcal{R}^2 = 1$  the ideal case in which the test-function agrees exactly with  $f(z)$ .

Test-function	$(A, B, C)$	$\mathcal{R}^2$
$f_1(z)$	(-3.897, 10.88, 7.185)	0.99974
$f_2(z)$	(-5.024, 8.651, 0.512)	0.99997
$f_3(z)$	(15.73, -9.286, 1.112)	0.99102
$f_4(z)$	(-3.152, -21.52, 1.114)	0.99630
$f_5(z)$	(-10.93, 3.173, 1.593)	0.99909
$f_6(z)$	(-3.463, 11.89, 4.143)	0.99959

TABLE I. Results of the  $\mathcal{R}^2$ -test on the test-functions Eqs. (39a)–(39f) using the parameters  $(\Omega_{m0}, h, q_0, j_0) = (0.289, 0.692, -0.545, 0.776)$ .

As an example, we consider the red curve of Fig. 1. The  $\mathcal{R}^2$ -test suggests that the most suitable choice corresponds to the function (39b) (see Table I), i.e.

$$f(z) = A + Bz^2 e^{Cz} \quad (42)$$

with

$$(A, B, C) = (-5.024, 8.651, 0.512). \quad (43)$$

However, it is evident from Table I that very good approximations for  $f(z)$  are also the functions Eq. (39a) and Eq. (39f), whose  $\mathcal{R}^2$  values are far from the best one by only 0.024% and 0.038%, respectively. The comparison between the numerical solution of  $f(z)$  and the functional form of Eq. (42) is shown in Fig. 2.

The second step takes  $H(z)$  up to the third order, restricting the value of the snap parameter to the interval [35]

$$s_0 \in [-1, 0]. \quad (44)$$

In this case, fixing  $(\Omega_{m0}, h, q_0, j_0)$  to the best-fit values, we show in Fig. 3 the behaviour of  $f(z)$  for different

values of  $s_0$ . Consistently with what found before, the best approximation for  $f(z)$  corresponding to the best-fit value of  $s_0$  is provided by the same function as in Eq. (42), but with slightly different free parameters, namely:

$$(A, B, C) = (-5.022, 8.577, 0.532). \quad (45)$$

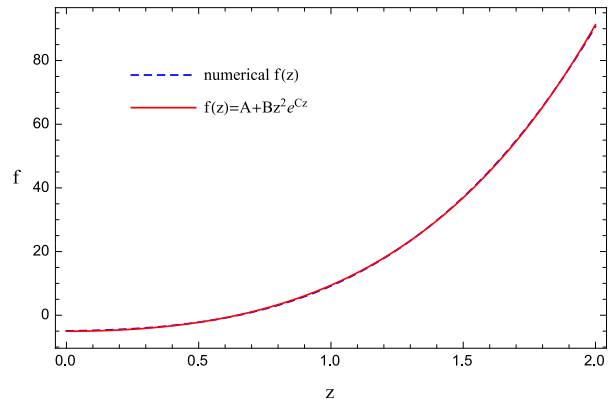


FIG. 2. Comparison between the numerical solution and the analytical approximation of  $f(z)$ . The parameters  $(\Omega_{m0}, h, q_0, j_0)$  are based on the best-fit results found in [31], while the coefficients  $(A, B, C)$  are given in Eq. (43).

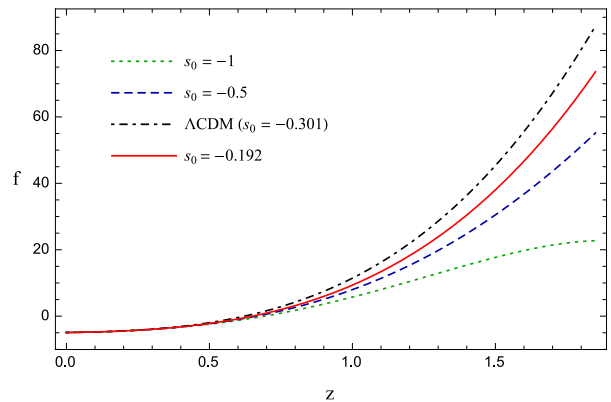


FIG. 3. Numerical solution of  $f(z)$  for different values of the snap parameter. The parameters  $(\Omega_{m0}, h, q_0, j_0)$  are based on the best-fit results found in [31]. The solid red line corresponds to the best-fit value of  $s_0$ . The dot-dashed black line corresponds to the  $\Lambda$ CDM model with  $\Omega_{m0} = 0.289$ .

## V. $f(T)$ COSMOLOGICAL MODELS

Our goal is now to reconstruct the function  $f(T)$  through a back-scattering procedure. In particular, inverting the expansion of  $H(z)$  up to the snap parameter by means of Eq. (16), one finds  $z$  in terms of  $T$ , which can be inserted back into Eq. (42) to finally reconstruct  $f(T)$ . To take into account the uncertainties in the es-

timate of the cosmographic parameters that may propagate through our numerical analysis, we rescale Eq. (42) as

$$\alpha f(z) \rightarrow f(z) , \quad (46)$$

where the constant  $\alpha$  will be determined from cosmological constraints. One obtains:

$$z(T) = \frac{1}{2\mathcal{Q}} \left[ 2(q_0^2 - j_0) + \left( \frac{4\mathcal{M}(T)}{H_0^3} \right)^{1/3} + \left( \frac{16H_0^3}{\mathcal{M}(T)} \right)^{1/3} \left( j_0^2 + q_0^2(6 + 12q_0 + 7q_0^2) - 2j_0(3 + 7q_0 + 5q_0^2) - 2s_0(1 + q_0) \right) \right] \quad (47)$$

and

$$f(T) = \alpha \mathcal{A} + \frac{\alpha \mathcal{B}}{4\mathcal{Q}^2} \left[ 2(q_0^2 - j_0) + \left( \frac{4\mathcal{M}(T)}{H_0^3} \right)^{1/3} + \left( \frac{16H_0^3}{\mathcal{M}(T)} \right)^{1/3} \left( j_0^2 + q_0^2(6 + 12q_0 + 7q_0^2) - 2j_0(3 + 7q_0 + 5q_0^2) - 2s_0(1 + q_0) \right) \right]^2 e^{\frac{c}{2\mathcal{Q}}} \left[ 2(q_0^2 - j_0) + \left( \frac{4\mathcal{M}(T)}{H_0^3} \right)^{1/3} + \left( \frac{16H_0^3}{\mathcal{M}(T)} \right)^{1/3} \left( j_0^2 + q_0^2(6 + 12q_0 + 7q_0^2) - 2j_0(3 + 7q_0 + 5q_0^2) - 2s_0(1 + q_0) \right) \right] \quad (48)$$

where

$$\mathcal{M}(T) \equiv H_0^2 \sqrt{2\mathcal{P}(T)} \mathcal{Q} - 2H_0^3 \mathcal{N} + \sqrt{-6T} H_0^2 \mathcal{Q}^2 , \quad (49)$$

$$\begin{aligned} \mathcal{P}(T) \equiv & 2H_0^2 \left[ 6j_0^3 - 6q_0^2(2 + q_0(4 + q_0))^2 + 3j_0^2(8 + q_0(28 + 17q_0)) + 4(2 + q_0(6 - q_0(3 + 7q_0)))s_0 + 9s_0^2 \right. \\ & \left. + 2j_0(6(2 + 3s_0) + q_0(52 + q_0(60 - q_0(6 + 17q_0)) + 27s_0)) \right] - 2\sqrt{-6T} H_0 (j_0^3 + 3j_0^2(1 + q_0)(6 + 11q_0) \\ & - 3j_0q_0^2(12 + q_0(29 + 16q_0)) + q_0^4(18 + q_0(36 + 17q_0)) - 15q_0^2(1 + q_0)s_0 + 3j_0(5 + 7q_0)s_0 + 3s_0^2) \\ & - 3T(-3q_0^2(1 + q_0) + j_0(3 + 4q_0) + s_0)^2 , \end{aligned} \quad (50)$$

$$\mathcal{Q} \equiv -3q_0^2(1 + q_0) + j_0(3 + 4q_0) + s_0 , \quad (51)$$

$$\begin{aligned} \mathcal{N} \equiv & j_0^3 + 3j_0^2(1 + q_0)(6 + 11q_0) - 3j_0q_0^2(12 + q_0(29 + 16q_0)) + q_0^4(18 + q_0(36 + 17q_0)) - 15q_0^2(1 + q_0)s_0 \\ & + 3j_0(5 + 7q_0)s_0 + 3s_0^2 . \end{aligned} \quad (52)$$

We can use the reconstructed  $f(T)$  to study  $\rho_T$  and  $p_T$  and their cosmological implications and to compare our

results with cosmological models developed in the literature so far [36]. So that, Eqs. (10a) and (10b) become:

$$\rho_T = -\frac{1}{2} \left[ T + \alpha \left( \mathcal{A} + \frac{\mathcal{B} \xi(T)}{4\mathcal{Q}^2} e^{\frac{c\xi(T)}{2\mathcal{Q}}} \right) \right] + \frac{2^{1/3} \alpha \mathcal{B} T G(T)}{24H_0^3 \mathcal{Q}^3 \mathcal{M}(T)^2} X(T) Y(T) \mathcal{M}'(T) e^{\frac{c\xi(T)}{2\mathcal{Q}}} , \quad (53)$$

$$\begin{aligned}
p_T = & \left[ e^{-\frac{c\xi(T)}{2\mathcal{Q}}} H_0^4 Q^4 \mathcal{M}(T)^{10/3} \left( 72\mathcal{A} + \frac{18\mathcal{B}\xi(T)^2}{Q^2} e^{\frac{c\xi(T)}{2\mathcal{Q}}} - \frac{3 \times 2^{1/3} \mathcal{B} T G(T) X(T) Y(T) \mathcal{M}'(T)}{H_0^3 Q^3 \mathcal{M}(T)^2} e^{\frac{c\xi(T)}{2\mathcal{Q}}} + \frac{2^{1/3} \mathcal{B} T^2}{H_0^3 Q^4 \mathcal{M}(T)^{10/3}} \right. \right. \\
& \times e^{\frac{c\xi(T)}{2\mathcal{Q}}} \left( 2^{1/3} \mathcal{C} G(T)^2 X(T) Y(T) \mathcal{M}'(T)^2 + 2^{7/3} H_0 \mathcal{Q} X(T) Y(T) \mathcal{M}(T) \mathcal{M}'(T)^2 + 2 H_0 \mathcal{Q} G(T) \mathcal{M}(T)^{1/3} \right. \\
& \times \left( -6 X(T) Y(T) \mathcal{M}'(T)^2 + 2^{5/3} (\mathcal{C} X(T) + Y(T)) \mathcal{M}(T)^{2/3} \mathcal{M}'(T)^2 + 2 H_0 ((2\mathcal{Q} + \mathcal{C}(q_0^2 - j_0)) X(T) \right. \\
& \left. \left. + (q_0^2 - j_0) Y(T)) \mathcal{M}(T)^{1/3} \mathcal{M}'(T)^2 + 3 X(T) Y(T) \mathcal{M}(T) \mathcal{M}''(T) \right) \right) \left. \right] \times \left[ 2^{4/3} \mathcal{B} \left( 2^{1/3} \mathcal{C} G(T)^2 X(T) Y(T) \mathcal{M}'(T)^2 \right. \right. \\
& \left. \left. + 2^{7/3} H_0 \mathcal{Q} T X(T) Y(T) \mathcal{M}(T) \mathcal{M}'(T)^2 + H_0 \mathcal{Q} G(T) \mathcal{M}(T)^{1/3} \left( -12 T X(T) Y(T) \mathcal{M}'(T)^2 + 2^{7/3} (\mathcal{C} X(T) \right. \right. \right. \\
& \left. \left. \left. + Y(T)) T \mathcal{M}(T)^{2/3} \mathcal{M}'(T)^2 + 4 H_0 ((2\mathcal{Q} + \mathcal{C}(q_0^2 - j_0)) X(T) + (q_0^2 - j_0) Y(T)) T \mathcal{M}(T)^{1/3} \mathcal{M}'(T)^2 \right. \right. \right. \\
& \left. \left. \left. + 3 X(T) Y(T) \mathcal{M}(T) (\mathcal{M}'(T) + 2 T \mathcal{M}''(T)) \right) \right) \right] \quad (54)
\end{aligned}$$

where

$$\xi(T) \equiv 2(q_0^2 - j_0) + \left( \frac{4\mathcal{M}(T)}{H_0^3} \right)^{1/3} + \left( \frac{16H_0^3}{\mathcal{M}(T)} \right)^{1/3}, \quad (55)$$

$$X(T) \equiv 2^{4/3} H_0^2 \mu + 2 H_0 (q_0^2 - j_0) \mathcal{M}(T)^{1/3} + 2^{2/3} \mathcal{M}(T)^{2/3}, \quad (56)$$

$$Y(T) \equiv 2^{4/3} \mathcal{C} H_0^2 \mu + 2 H_0 (2\mathcal{Q} + \mathcal{C}(q_0^2 - j_0)) \mathcal{M}(T)^{1/3} + 2^{2/3} \mathcal{C} \mathcal{M}(T)^{2/3}, \quad (57)$$

$$G(T) \equiv -2 H_0^2 \mu + 2^{1/3} \mathcal{M}(T)^{2/3} \quad (58)$$

$$\mu \equiv j_0^2 + q_0^2(6 + 12q_0 + 7q_0^2) - 2j_0(3 + 7q_0 + 5q_0^2) - 2s_0(1 + q_0) \quad (59)$$

and

$$\mathcal{M}'(T) \equiv \frac{\partial \mathcal{M}(T)}{\partial T} = \frac{1}{\sqrt{2}} \left[ \frac{\sqrt{3} H_0^2 \mathcal{Q}^2 T}{(-T)^{3/2}} + \frac{H_0^2 \mathcal{Q}}{\sqrt{\mathcal{P}(T)}} \mathcal{P}'(T) \right], \quad (60)$$

$$\mathcal{M}''(T) \equiv \frac{\partial^2 \mathcal{M}(T)}{\partial T^2} = -\frac{\sqrt{-3T} H_0^2 \mathcal{Q}^2 \mathcal{P}(T)^2 + H_0^2 \mathcal{Q} T^2 \mathcal{P}(T)^{1/2} \mathcal{P}'(T)^2 - 2 H_0^2 \mathcal{Q} T^2 \mathcal{P}(T)^{3/2} \mathcal{P}''(T)}{2\sqrt{2} T^2 \mathcal{P}(T)^2}, \quad (61)$$

$$\begin{aligned}
\mathcal{P}'(T) \equiv \frac{\partial \mathcal{P}(T)}{\partial T} = & -3(-3q_0^2(1 + q_0) + j_0(3 + 4q_0) + s_0)^2 + \frac{\sqrt{6} H_0}{\sqrt{-T}} \left[ j_0^3 + 3j_0^2(1 + q_0)(6 + 11q_0) - 3j_0 q_0^2(12 \right. \\
& \left. + q_0(29 + 16q_0) + q_0^4(18 + q_0(36 + 17q_0) - 15q_0^2(1 + q_0)s_0) + 3j_0(5 + 7q_0)s_0 + 3s_0^2 \right], \quad (62)
\end{aligned}$$

$$\begin{aligned}
\mathcal{P}''(T) \equiv \frac{\partial^2 \mathcal{P}(T)}{\partial T^2} = & \sqrt{\frac{3}{2}} \frac{H_0}{(-T)^{3/2}} \left[ j_0^3 + 3j_0^2(1 + q_0)(6 + 11q_0) - 3j_0 q_0^2(12 + q_0(29 + 16q_0)) + q_0^4(18 + q_0(36 + 17q_0)) \right. \\
& \left. - 15q_0^2(1 + q_0)s_0 + 3j_0(5 + 7q_0)s_0 + 3s_0^2 \right]. \quad (63)
\end{aligned}$$

We notice that  $p_T$  is in fact independent of the rescaling factor  $\alpha$ . From the condition of having an accelerating

expansion today, we are able to constrain  $\alpha$  by imposing



that  $\omega_{DE} < -1/3$ . Thus,

$$0 < \alpha \lesssim 0.936 . \quad (64)$$

Fig. 4 shows the reconstructed  $f(T)$  for the best-fit values of the cosmographic parameters with the indicative value of  $\alpha = 0.5$ . The physical density  $\rho_T$  and pressure  $p_T$  are

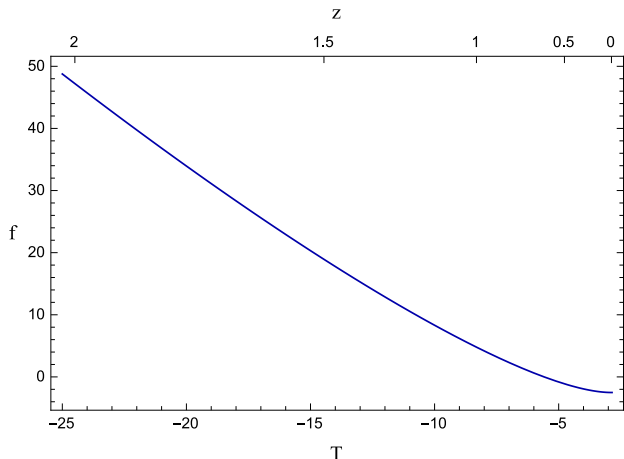


FIG. 4. Reconstructed  $f(T)$  for the best-fit values of the cosmographic parameters and  $\alpha = 0.5$  in the redshift range  $0 \leq z \leq 2$ .

shown in Figs. 5 and 6 , respectively, while we show in Fig. 7 the effective dark energy EoS parameter as defined in Eq. (13).

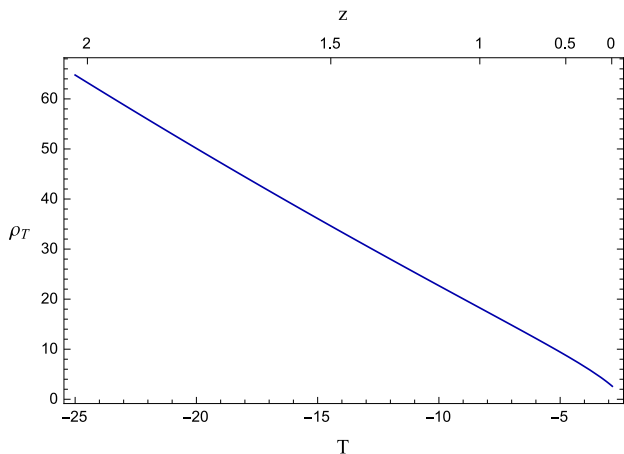


FIG. 5. Torsion density for the best-fit values of the cosmographic parameters and  $\alpha = 0.5$  in the redshift range  $0 \leq z \leq 2$ .

## VI. COMPARING $f(T)$ MODELS

In this section, we compare the reconstructed  $f(T)$  model with the one proposed in [22], which has been obtained by means of cosmography. Both the approaches might be in agreement to guarantee the goodness of our

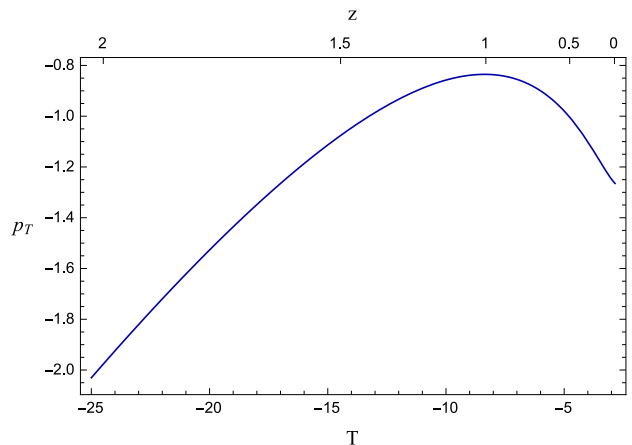


FIG. 6. Torsion pressure for the best-fit values of the cosmographic parameters in the redshift range  $0 \leq z \leq 2$ .

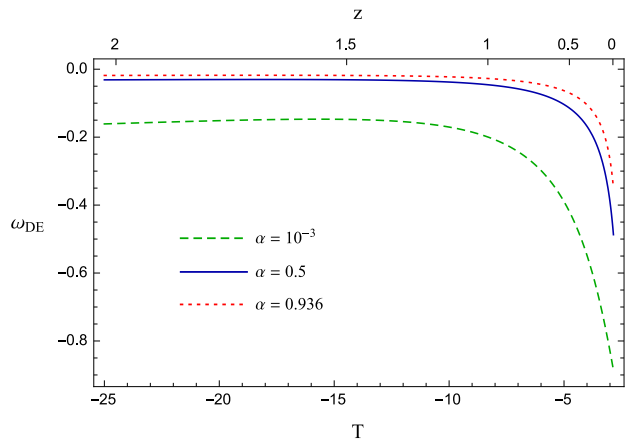


FIG. 7. Effective dark energy EoS parameter for the best-fit values of the cosmographic parameters in the redshift range  $0 \leq z \leq 2$ . The different curves correspond to different values of the rescale factor  $\alpha$  (cf. Eq. (64)).

numerical analysis, in the redshift domain in which cosmography is valid. So that, let us recall the model defined in [22]

$$f(T)_{\text{ABCL}} = c_0 T + (T - T_0) \left[ c_1 + c_3 \cosh(T - T_0) + (T - T_0) \left( c_2 + c_4 (T - T_0) \sinh(T - T_0) \right) \right] \quad (65)$$

where  $T_0 = -6H_0^2$ . The model is composed by distinct parts, each of them dominates over the other as the redshift increases. In particular, we choose the free parameters  $c_i$  ( $i = 0, \dots, 4$ ) imposing that  $f(T_0) = 6H_0^2(\Omega_{m0} - 2)$  and  $f'(T_0) = 1$ , as well as we made as initial settings of our approach. So that, by using the derivative constraints on  $f(T)$  at  $z = 0$ , obtained from a direct experimental

analysis with different data sets, one gets:

$$c_0 = 2 - \Omega_{m0} \quad (66a)$$

$$c_1 = \Omega_{m0} - 1 \quad (66b)$$

$$c_2 = -3 \times 10^{-6} \quad (66c)$$

$$c_3 = \frac{1}{15} \times 10^{-9} \quad (66d)$$

$$c_4 = \frac{3}{4} \times 10^{-14} \quad (66e)$$

while the best-fit values of the present matter density parameter and the Hubble constant were found to be, respectively

$$\Omega_{m0} = 0.364, \quad H_0 = 71.47 \text{ km/s/Mpc}. \quad (67)$$

Without taking into account the sign of  $T$ , let us consider the comparison between our present model and Eq. (65). It is clear, from Fig. 8, that the two models are compatible for  $z \leq 1$ . Discrepancies have been accounted since the previous model has been obtained by means of heuristic results due to cosmography, whereas our model is a numerical solution of the modified Friedmann equations. Discrepancies are around the 10% ÷ 15% and testify the goodness between the two approaches. We conclude that both the models are similar to the concordance paradigm and seem to slightly depart from it at the observable limit of  $z > 1$ . More significant deviations are however available as one exceeds such an interval, i.e. for  $z > 1$ . The limit of cosmography, found in the model (65) is overcome by extending it with the numerical analysis performed in the present work.

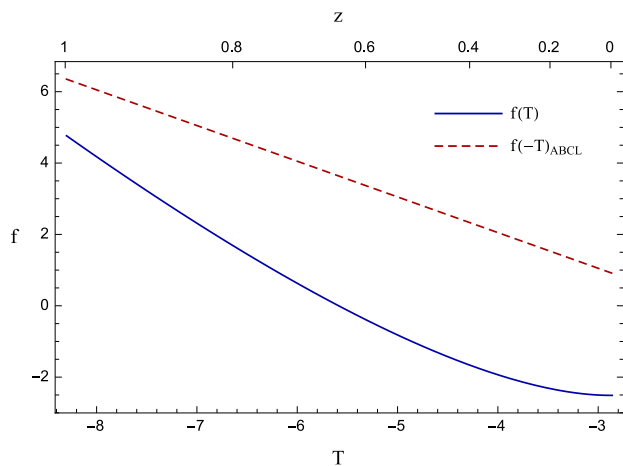


FIG. 8. Comparison between  $f(T)$  found in this work for  $\alpha = 0.5$  (solid blue line) and  $f(|T|)$  proposed in [22] (dashed red line) in the redshift interval  $0 \leq z \leq 1$ .

## VII. CONCLUSIONS

We considered  $f(T)$  teleparallel cosmological models. In particular, we proposed a new model-independent

strategy to reconstruct the  $f(T)$  function, without *a priori* assumptions over the model. To figure out this, we recast the Hubble parameter  $H(z)$  in terms of cosmographic parameters and expanded it up to the jerk first and snap later. We noticed that our outcomes have not been influenced by the order, leaving unaltered the functional behaviors of  $f(T)$ . So, since numerical bounds over the cosmographic series can be found from kinematics only, without requiring any other assumptions, we rewrote the modified Friedmann equations in terms of the redshift only and recast  $f(T)$  as function of the redshift  $z$  through the constraint  $T = -6H^2$ , with  $H = H(z)$ , previously expanded in Taylor series. In particular, we set the cosmographic parameters by means of the most recent observations first, and, later, with the concordance  $\Lambda$ CDM predictions.

Our treatment enabled us to get a single set of differential equations all in terms of the redshift, which can be numerically solved in order to get  $f(z) \equiv f(T(H))$ . So that, using the most recent bounds over the cosmographic coefficients, we inferred  $f(z)$  through test-functions. All the adopted test functions passed the cosmographic initial settings and framed the universe dynamics with a precise accuracy. We handled several test-functions and found that the best agreement can be accounted if  $f(z) = \mathcal{A} + \mathcal{B}z^2e^{\mathcal{C}z}$ . In this perspective, we considered a statistical  $\mathcal{R}^2$ -test, to get the significance between our model and the proposed test-functions. We thus found the set of free parameters to be  $(\mathcal{A}, \mathcal{B}, \mathcal{C}) = (-5.022, 8.577, 0.532)$  and noticed that  $f(z)$  is neither odd nor even, being constructed without linear terms  $\propto z$ . Afterwards, we came back to  $f(T)$  and its evolution in terms of  $T$ , with a backscattering procedure, i.e. inverting  $z$  in terms of  $T$ , by means of  $T = -6H^2$ . Therefore, we investigated some consequences of the obtained  $f(T)$  model and wrote its equation of state, which turns out to be different from the concordance case, providing a slightly varying effective dark energy term. Finally, we compared our results with the ones proposed in previous cosmographic  $f(T)$  models. We showed that, at least in the redshift domain  $z \in [0, 1]$ , the approach that made use of cosmography agrees with our prescription. Outer this interval, however, the effective dark energy term turns out to be consistently different from a pure cosmological constant, providing that the  $\Lambda$ CDM model can be seen as a limit of a more general paradigm included in  $f(T)$  gravity cosmologies. Future works will include refined numerical tests in view to extend the numerical behaviors of  $f(z)$  toward early phase cosmology at higher  $z$ .

## ACKNOWLEDGMENTS

S.C. acknowledges the support of INFN (iniziativa specifica QGSKY). This paper is based upon work from COST action CA15117 (CANTATA), supported by COST (European Cooperation in Science and Technology).

- [1] K. Bamba, S. Capozziello, S. Nojiri and S. D. Odintsov, *Astrophys. Space Sci.*, **342**, 155 -228, (2012); T. M. Davis, D. Parkinson, *Handb. Super.*, **1**, (2016); A. Joyce, L. Lombriser, F. Schmidt, *Annu. Rev. Nucl. Part. Sci.*, **66**, 95-122, (2016); K. Kleidis, N. K. Spyrou, *Entropy*, **18**, 3-94, (2016).
- [2] A. G. Riess et al., *Astron. J.*, **116**,1009-1038, (1998); S. Perlmutter et al., *Astrophys. J.*, **517**, 565- 586, (1999).
- [3] P. A. R. Ade et al. *Planck 2015 results. XIII. Cosmological parameters*, *Astron. Astrophys.*, **594**, A13, (2016).
- [4] E. J. Copeland, M. Sami, S. Tsujikawa, *Int. J. Mod. Phys. D*, **15**, 1753, (2006); S. Perlmutter et al., *Nature*, **391**, 51-54, (1998); B. P. Schmidt et al., *Astrophys. J.*, **507**, 46-63, (1998); A. G. Riess, et al., *Astrophys. J.*, **607**, 665-687, (2004).
- [5] P. J. E. Peebles, B. Ratra, *Rev. Mod. Phys.*, **75**, 559-606, (2003); L. Amendola, M. Kunz, M. Motta, I. D. Saltas and I. Sawicki, *Phys. Rev. D*, **87**, 023501, (2013).
- [6] I. Zlatev, L. M. Wang, and P. J. Steinhardt, *Phys. Rev. Lett.*, **82**, 896-899, (1999).
- [7] S. Weinberg, *Rev. Mod. Phys.*, **61**, 1, (1989); S. Tsujikawa, ArXiv[astro-ph]:1004.1493, *Dark energy:investigation and modeling*; C. P. Burgess, ArXiv[hep-th]:1309.4133, *The Cosmological Constant Problem: Why its hard to get Dark Energy from Micro-physics*, (2013).
- [8] S. Capozziello, M. De Laurentis, *Phys. Rept.*, **509**, 167, (2011); L. M. Krauss, J. Dent, *Phys. Rev. Lett.*, **111**, 061802, (2013).
- [9] S. Capozziello, M. Francaviglia, *Gen.Rel. Grav.*, **40**, 357 (2008).
- [10] A. De Felice and S. Tsujikawa, *Living Rev. Rel.*, **13**, 3, (2010).
- [11] S. Nojiri, S.D. Odintsov, *Phys. Rept.*, **505**, 59, (2011).
- [12] A. Einstein 1928, *Sitz. Preuss. Akad. Wiss.* p. 217; *ibid* p. 224; A. Unzicker and T. Case, *physics/0503046*; R. Aldrovandi and J. G. Pereira, *Teleparallel Gravity: An Introduction*, (Springer, Dordrecht, 2013); J. W. Maluf, *Annalen Phys.*, **525**, 339, (2013).
- [13] R. Ferraro, F. Fiorini, *Phys. Rev. D*, **75**, 084031, (2007); *Phys. Rev. D*, **78**, 124019, (2008).
- [14] E. V. Linder, *Phys. Rev. D*, **81**, 127301, (2010) [Erratum-*ibid.* D, **82**, 109902, (2010)].
- [15] Y. F. Cai, S. Capozziello, M. De Laurentis, E. N. Saridakis, *Rept. Prog. Phys.*, **79**, 10, 106901, (2016).
- [16] P. Wu, H. W. Yu, *Phys. Lett. B*, **693**, 415, (2010); S. H. Chen, J. B. Dent, S. Dutta, E. N. Saridakis, *Phys. Rev. D* **83**, 023508 (2011); J. B. Dent, S. Dutta, E. N. Saridakis, *JCAP*, **1101**, 009 (2011); K. Bamba, R. Myrzakulov, S. i. Nojiri and S. D. Odintsov, *Phys. Rev. D* **85**, 104036 (2012); G. Otalora, *JCAP*, **1307**, 044 (2013); K. Izumi and Y. C. Ong, *JCAP*, **1306**, 029 (2013).
- [17] K. Bamba, C. Q. Geng, C. C. Lee, L. W. Luo, *JCAP*, **1101**, 021, (2011); M. Sharif, S. Rani, *Mod. Phys. Lett. A*, **26**, 1657 (2011); M. R. Setare, M. J. S. Houndjo, *Can. J. Phys.*, **91**, 260-267, (2012); J. Amoros, J. de Haro and S. D. Odintsov, *Phys. Rev. D* **87**, 104037 (2013); G. G. L. Nashed and W. El Hanafy, *Eur. Phys. J. C* **74**, no. 10, 3099 (2014); V. Fayaz, H. Hossienkhani, A. Farmany, M. Amirabadi and N. Azimi, *Astrophys. Space Sci.* **351**, 299 (2014).
- [18] P.J.E. Peebles, *Principles of Physical Cosmology*, Princeton Univ. Press, (1993).
- [19] S. Capozziello, O. Luongo, E. N. Saridakis, *Phys. Rev. D*, **91**, 124037, (2015).
- [20] S. Capozziello, M. De Laurentis, O. Luongo, A. C. Ruggeri, *Galaxies*, **1**, 216-260, (2013).
- [21] S. Capozziello, V.F. Cardone, V. Salzano, *Phys. Rev. D*, **78**, 063504 (2008).
- [22] A. Aviles, A. Bravetti, S. Capozziello, O. Luongo, *Phys. Rev. D*, **90**, 0403531, (2014).
- [23] E. Harrison, *Nature*, **260**, 591, (1976); M. Visser, *Phys. Rev. D*, **56**, 7578, (1997).
- [24] M. Visser, *Gen. Rel. Grav.*, **37**, 1541, (2005); M. Visser, *Class. Quant. Grav.*, **32**, 135007, (2015); O. Luongo, *Mod. Phys. Lett. A*, **28**, 1350080, (2013).
- [25] V. C. Busti, A. de la Cruz-Dombriz, P. K. S. Dunsby and D. Saz-Gmez, *Phys. Rev. D*, **92**, 123512, (2015); M. Demianski, E. Piedipalumbo, C. Rubano, P. Scudellaro, *Mon. Not. Roy. Astron. Soc.*, **426**, 1396, (2012).
- [26] A. Aviles, C. Gruber, O. Luongo, H. Quevedo, *Phys. Rev. D*, **86**, 123516, (2012);
- [27] Orlando Luongo, *Mod. Phys. Lett. A*, **26**, 20, 1459-1466, 8, (2011); O. Luongo, G. B. Pisani, A. Troisi, *Int. Jour. Mod. Phys. D*, **26**, 1750015, 10, (2017).
- [28] C. Gruber, O. Luongo, *Phys. Rev. D*, **89**, 103506, (2014).
- [29] P. K. S. Dunsby, O. Luongo, *Int. J. Geom. Meth. Mod. Phys.*, **13**, 03, 1630002, (2016).
- [30] O. Luongo, *Mod. Phys. Lett. A*, **26**, 1459, (2011).
- [31] A. de la Cruz-Dombriz, P. K. S. Dunsby, O. Luongo, L. Reverberi, *JCAP*, **12**, 1612, 042, (2016).
- [32] R. C. Nunes, A. Bonilla, S. Pan, E. N. Saridakis, *Eur. Phys. J. C*, **77**, 4, 230, (2017); R. C. Nunes, S. Pan, E. N. Saridakis, *JCAP*, **1608**, 08, 011, (2016).
- [33] D. Muthukrishna, D. Parkinson, *JCAP*, **1611**, 052, (2016); H. Jennen, J. G. Pereira, *Phys. Dark Univ.*, **11**, 49, (2016).
- [34] N. R. Draper, H. Smith, *Applied Regression Analysis*, Wiley-Interscience, (1998).
- [35] Y. N. Zhou, D. Z. Liu, X. B. Zou, H. Wei, *Eur. Phys. J. C*, **76**, 5, 281, (2016); M. Visser, *Class. Quant. Grav.*, **32**, 13, 135007, (2015); A. Aviles, A. Bravetti, S. Capozziello, O. Luongo, *Phys. Rev. D*, **90**, 4, 043531, (2014); M. Moresco, L. Pozzetti, A. Cimatti, R. Jimenez, C. Maraston, L. Verde, D. Thomas, A. Citro, R. Tojeiro, D. Wilkinson, *JCAP*, **05**, 1605, 014, (2016).
- [36] S. Nesseris, S. Basilakos, E. N. Saridakis, L. Perivolaropoulos, *Phys. Rev. D*, **88**, 103010, (2013).